

## Computational Study of Thioflavin T Torsional Relaxation in the Excited State

Vitali I. Stsiapura\* and Alexander A. Maskevich

Yanka Kupala State University, Physics Department, 22 Ozheshko Street, 230023 Grodno, Belarus

Valery A. Kuzmitsky

Institute of Molecular and Atomic Physics, National Academy of Sciences of Belarus, Nezavisimosti Avenue 70, 220072 Minsk, Belarus

Konstantin K. Turoverov and Irina M. Kuznetsova

Institute of Cytology, Russian Academy of Sciences, St. Petersburg 197376, Russia

Received: January 23, 2007; In Final Form: April 2, 2007

Quantum-chemical calculations of the Thioflavin T (ThT) molecule in the ground  $S_0$  and first excited singlet  $S_1$  states were carried out. It has been established that ThT in the ground state has a noticeable nonplanar conformation: the torsion angle  $\varphi$  between the benzothiazole and the dimethylaminobenzene rings has been found to be  $\sim 37^\circ$ . The energy barriers of the intramolecular rotation appearing at  $\varphi = 0$  and  $90^\circ$  are quite low: semiempirical AM1 and PM3 methods predict values  $\sim 700$   $\text{cm}^{-1}$  and ab initio methods  $\sim 1000$ – $2000$   $\text{cm}^{-1}$ . The INDO/S calculations of vertical transitions to the  $S_1^{(\text{abs})}$  excited state have revealed that energy  $E_{S_1^{(\text{abs})}}$  is minimal for the twisted conformation with  $\varphi = 90^\circ$  and that the intramolecular charge-transfer takes place upon the ThT fragments' rotation from  $\varphi = 0$  to  $90^\circ$ . Ab initio CIS/RHF calculations were performed to find optimal geometries in the excited  $S_1$  state for a series of conformers having fixed  $\varphi$  values. The CIS calculations have predicted a minimum of the  $S_1$  state energy at  $\varphi \sim 21^\circ$ ; however, the energy values are 1.5 times overestimated in comparison to experimental data. Excited state energy dependence on the torsion angle  $\varphi$ , obtained by the INDO/S method, reveals that  $E_{S_1^{(\text{fluor})}}$  is minimal at  $\varphi = \sim 80$ – $100^\circ$ , and a plateau is clearly observed for torsion angles ranging from 20 to  $50^\circ$ . On the basis of the calculation results, the following scheme of photophysical processes in the excited  $S_1$  state of the ThT is suggested. According to the model, a twisted internal charge-transfer (TICT) process takes place for the ThT molecule in the excited singlet state, resulting in a transition from the fluorescent locally excited (LE) state to the nonfluorescent TICT state, accompanied by torsion angle  $\varphi$  growth from 37 to  $90^\circ$ . The TICT process effectively competes with radiative transition from the LE state and is responsible for significant quenching of the ThT fluorescence in low-viscosity solvents. For viscous solvents or when the ThT molecule is located in a rather rigid microenvironment, for example, when it is bound to amyloid fibrils, internal rotation in the dye molecule is blocked due to steric hindrance, which results in suppression of the  $\text{LE} \rightarrow \text{TICT}$  quenching process and in a high quantum yield of fluorescence.

### Introduction

Association of proteins into ordered, filamentous structures, commonly known as amyloid fibrils,<sup>1,2</sup> and deposition and accumulation of such aggregates in organism tissues lead to a number of serious diseases, such as neurodegenerative Alzheimer's and Parkinson's diseases, cataracts, etc.<sup>1,3–6</sup> Thioflavin T (ThT) (Figure 1) forms a highly fluorescent complex with amyloid fibrils and is widely used for their detection.<sup>7–10</sup> It was reported that the intensity of ThT emission selectively increased by several orders in the presence of amyloid fibrils.<sup>8</sup> Importantly, ThT does not interact with folded or partially folded monomeric proteins, soluble oligomers, or amorphous aggregates, or interaction of ThT with these species is not accompanied by noticeable changes in its fluorescence.<sup>7,8</sup>

However, in spite of the wide applications of this probe for detection purposes, the underlying mechanism of the dramatic

changes in fluorescence quantum yield (QY) upon ThT binding to amyloid fibrils is still unclear. Several explanations of ThT fluorescence properties were proposed. The formation of ThT dimers<sup>11,12</sup> or micelles<sup>13</sup> was suggested to be responsible for fluorescence intensity alteration. A weak point of this hypothesis is a low probability of dimerization or aggregation due to the nonzero positive charge of the dye. Furthermore, it has been already emphasized<sup>14</sup> that some erroneous conceptions related to the ThT spectral properties were due to the poor choice of experimental conditions and presence of impurities.

On the other hand, it was reported that the QY of ThT fluorescence depended mainly on viscosity rather than on the polarity or protic properties of solvents,<sup>14–16</sup> and the growth of viscosity or rigidity of the microenvironment resulted in a significant QY increase. It has been suggested that photoinduced intramolecular charge transfer takes place for the fluorophore<sup>14</sup> and that ThT behaves as a molecular rotor.<sup>14,15,17</sup>

The most prominent feature of the compounds referred to as molecular rotors<sup>18–22</sup> is the significant fluorescence increase

\* To whom correspondence should be addressed. Tel.: +375-152-743414. Fax: +375-152-731910. E-mail: stepuro@grsu.by.

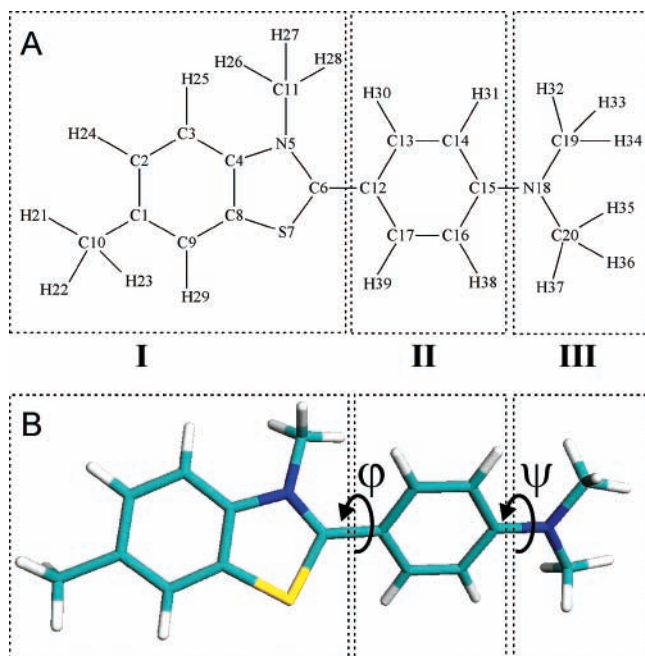


**Figure 1.** Chemical structure (A) and spatial model (B) of ThT cation. S, C, and N atoms are shown in yellow, cyan, and blue, respectively. Benzthiazole ring (I), benzene ring (II), and dimethylamino group (III) are boxed.

upon introduction into high-viscosity media due to the decreased torsional relaxation in the molecule. Internal rotation of molecular groups or fragments is associated with intramolecular charge-transfer processes,<sup>20,22</sup> leading to transitions from the fluorescent locally excited (LE) state to the nonfluorescent twisted internal charge-transfer (TICT) state.

Detailed information about the structure and molecular properties of ThT in the ground and excited states is needed to obtain insight on photophysical processes in the molecule. The present work was initiated to provide this information and establish the mechanism of the unique sensitivity of the dye emission to amyloid fibril presence.

### Computational Methods

Semiempirical AM1<sup>23</sup> and PM3<sup>24</sup> and ab initio methods (basis sets 3-21G<sup>25</sup> and 6-31G<sup>26</sup>) were used to calculate the geometry and energy of the ThT cation ( $Z = +1$ ) in the ground  $S_0$  state. A more accurate description of the conformers corresponding to the minima and the saddle points on the potential energy surface was achieved by the additional geometry optimization using an extended 6-31G(d,p)<sup>27</sup> basis set, which includes d orbitals for C, N, and S atoms and p orbitals for H atoms. Electron correlation effects were taken into account using the Møller–Plesset second-order perturbation theory method (MP2) as described earlier.<sup>28</sup>

The ThT geometry in the excited singlet state  $S_1$  was calculated using a configuration interaction with the singles (CIS) method<sup>29</sup> using 3-21G and 6-31G basis sets. A relatively large molecular size of ThT imposed significant computational difficulties when more accurate multiconfigurational (MCSCF)<sup>30</sup> or coupled-cluster<sup>31</sup> methods were applied. Therefore, we limited our investigations of excited state geometries to the CIS/RHF level only. A comparison of excited state energies calculated by this ab initio method with experimental data showed that the CIS method gave overestimated values.<sup>32–35</sup> Nevertheless, geometries obtained at the CIS level as well as molecular properties are quite reasonable and correct, at least as a first

approximation for a variety of organic and inorganic molecules.<sup>32,36–40</sup> In particular, such a conclusion was made for dimethylaminobenzonitrile,<sup>41</sup> a molecule that underwent intramolecular charge transfer accompanied by twisting<sup>42</sup> in the excited state.

Excited state properties (energies, oscillator strengths of electronic transitions) for ThT conformers were obtained using semiempirical method INDO/S,<sup>43</sup> taking into account the configuration interaction of five occupied and five unoccupied molecular orbitals. Charge redistribution among molecular fragments upon transition of the molecule to the excited state was calculated using transition density matrix formalism.<sup>44,45</sup>

All calculations (with the exception of INDO/S) were performed using the PC Gamess 6.3<sup>46</sup> and Wingamess (version R2, December 12, 2003) versions of the Gamess-US quantum-chemistry package.<sup>47</sup> The energies of the excited states, charge-transfer probabilities, and oscillator strengths of the electronic transitions were calculated using a set of programs developed by one of us (V.A.K). Conformer geometries and the molecular orbitals were visualized using the Molekel<sup>48</sup> and ArgusLab<sup>49</sup> programs.

### Results and Discussion

The structure of ThT is represented in Figure 1. The molecule can be divided into three fragments of chemical significance: the benzthiazole ring (fragment I), the benzene ring (fragment II), and the dimethylamino group (fragment III). These three groups are rather rigid, and one can expect that both structure and photophysical behavior of ThT should be determined mainly by their spatial orientations. Taking into account these assumptions, we selected two torsion angles,  $\varphi$  (N5–C6–C12–C13) and  $\psi$  (C14–C15–N18–C19), to detect and analyze probable conformations of ThT in the ground state. These torsion angles  $\varphi$  and  $\psi$  define spatial orientations of fragment II relative to fragment I and of fragment III relative to fragment II, respectively (Figure 1).

Other parameters of molecular geometry (except  $\varphi$  and  $\psi$ ) are denoted as a set of the parameters  $\omega$ . Hereinafter, we designate parameters, optimal for the ground  $S_0$  state, as  $\omega = \omega_0$  and for the first excited singlet state as  $\omega = \omega_1$ .

At a first stage, optimization of ThT geometry at fixed  $\varphi$  and  $\psi$  angles, ranging from 0 to 360° with a step of 30°, was carried out using semiempirical methods AM1 and PM3 to detect conformations with minimal energy. Parameters  $\omega$  were allowed to vary during the conformation search. These calculations gave the dependence of the ground state energy  $E_{S_0}(\varphi, \psi, \omega_0)$  on the  $\varphi$  and  $\psi$  angles (Figure 2). One can see eight minima on the energy surface, which correspond to stable conformations with almost identical energies at  $\varphi = 37, 145, 217, \text{ or } 325^\circ$  and  $\psi = 0 \text{ or } 180^\circ$ .

Thus, the computations show that benzthiazole and benzene fragments are not coplanar in the ground state and that the angle between their planes is equal to  $\varphi = \sim 37^\circ$  (small nonplanar distortion of the rings can be neglected). Minima of the  $E_{S_0}(\varphi, \psi, \omega_0)$  function at  $\varphi = 37, 145, 217, \text{ or } 325^\circ$  (Figure 2B) appear to be due to steric interactions of the benzthiazole methyl group with hydrogen atoms of benzene (fragment II). Substitution of the methyl group at the N5 atom with hydrogen is expected to result in a planar conformation of the molecule with a common  $\pi$  electronic system. Semiempirical AM1 calculations confirm the assumption made—for this case, the energy of the ground  $S_0$  state achieves its minimal value for planar conformations with  $\varphi = 0 \text{ or } 180^\circ$ .

Figure 2C shows that the dimethylamino group and the benzene ring of the ThT molecule are coplanar in the ground

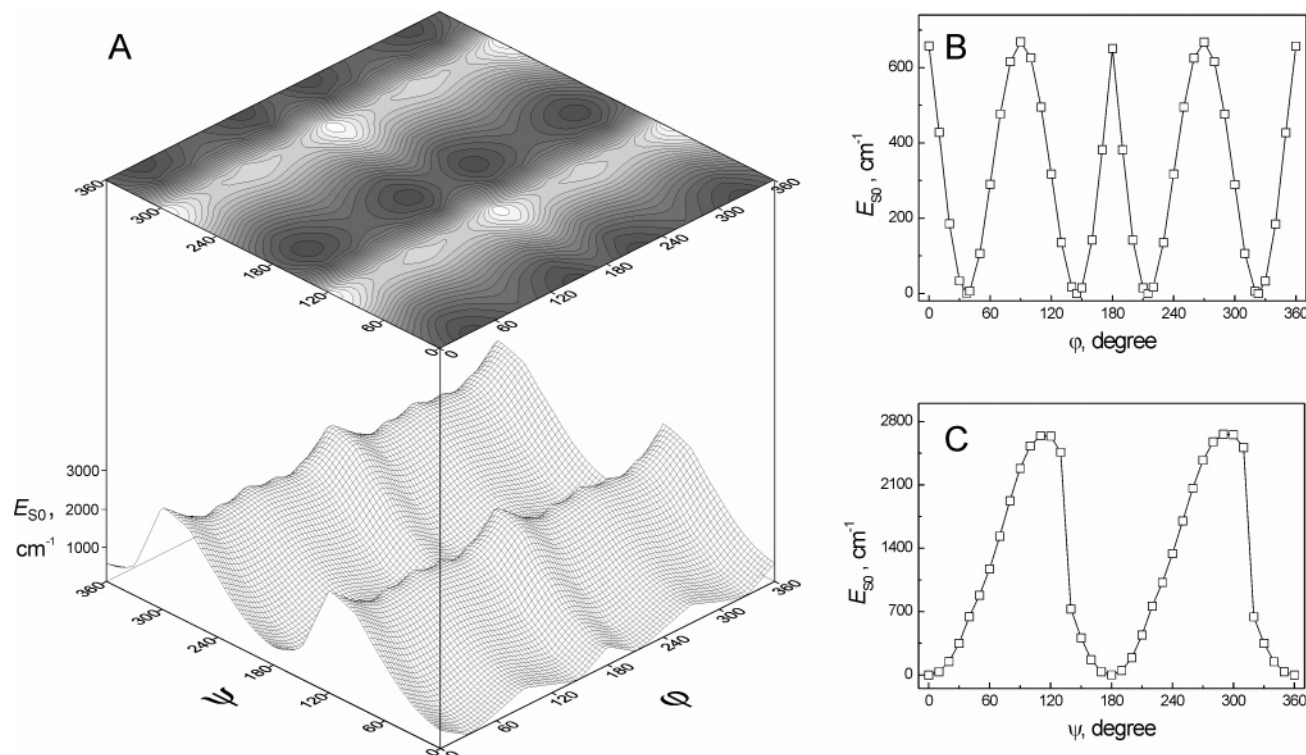


**Figure 2.** Dependence of ThT ground state energy on  $\varphi$  and  $\psi$  angle values. (A) Energy surface  $E_{S_0}(\varphi, \psi, \omega_0)$  vs  $\varphi$  and  $\psi$ . (B) Energy dependence on  $\varphi$  angle ( $\psi$  was allowed to vary). (C) Energy dependence on  $\psi$  angle ( $\varphi$  was allowed to vary). Calculations with AM1 method.

**TABLE 1: Ground State Energy and Dipole Moments for Selected ThT Conformers**

calculation method	$\varphi_{\min}^a$ (deg)	$E(\varphi = 0) - E(\varphi_{\min})$ ( $\text{cm}^{-1}$ )	$E(\varphi = 90) - E(\varphi_{\min})$ ( $\text{cm}^{-1}$ )	$\mu(\varphi = 0)$ (D)	$\mu(\varphi_{\min})$ (D)	$\mu(\varphi = 90)$ (D)
AM1	37.0	660	670	1.8	1.4	2.2
PM3	32.2	410	720	2.9	2.2	4.1
RHF/3-21G	37.0	1220	1560	3.8	3.1	3.1
RHF/6-31G	37.4	1250	1520	3.5	2.9	3.2
RHF/6-31G(d,p)	41.5	1550	1080	3.1	2.4	2.8
MP2/RHF/6-31G	43.6	1500	1180	3.6	2.8	3.1
MP2/RHF/6-31G(d,p)	45.6	2080	1450	2.7	2.0	2.6

<sup>a</sup> Torsion angle for the stable conformation in the  $S_0$  state.

state with  $\psi = 0$  or  $180^\circ$ , which is caused by the conjugation effects. It must be noted that upon dimethylamino group rotation, its planarity is distorted, leading to non-symmetrical shapes of barriers in the energy profile versus  $\psi$  angle.

Because of the symmetry of a potential energy profile along the torsion angles  $\varphi$  and  $\psi$ , we may limit our further calculations only to the  $0$ – $180^\circ$  interval. We have established that the energy barrier (Figure 2B and Table 1) between the neighboring minima on the potential energy surface  $E_{S_0}(\varphi, \psi, \omega_0)$  associated with the change in the torsion angle  $\varphi$  and correspondent to mutual rotation of the fragments I and II along the C6–C12 bond is relatively low,  $\Delta E = \sim 700 \text{ cm}^{-1}$  (AM1 method). The value of the potential barrier corresponding to rotation of the dimethylamino group relative to the benzene ring is roughly 4 times higher  $\Delta E = \sim 2800 \text{ cm}^{-1}$  (Figure 2C).

Qualitatively similar results were obtained using semiempirical PM3 and ab initio methods with basis sets 3-21G and 6-31G (Figure 3A and Table 1). In the latter case, the potential barrier of the fragments I and II rotation along the C6–C12 bond is higher ( $\Delta E = \sim 1200$ – $1300 \text{ cm}^{-1}$  at angles  $\varphi = 0$  or  $180^\circ$  and  $\Delta E = \sim 1500 \text{ cm}^{-1}$  at  $\varphi = 90$  or  $270^\circ$ ). However, for an extended basis set 6-31G(d,p) or when correlation effects are taken into account using the MP2 method (Table 1), the barrier energies noticeably decrease for conformers with  $\varphi = \sim 90^\circ$  (or  $270^\circ$ ) and increase for conformers with  $\varphi = \sim 0^\circ$  (or  $180^\circ$ ). Moreover, values of the angle  $\varphi$  for stable conformers

become slightly larger. Nevertheless, we can conclude that even calculations with the 3-21G basis set reproduce the features of the ground state energy profile rather well.

It is noteworthy that stable conformers possess smaller dipole moments than conformers near saddle points on potential energy profiles (Table 1, Supporting Information). Therefore, one may expect that the barriers' heights for mutual rotation of fragments I and II will be even lower for ThT in polar solvents.

Although the barriers on the  $E_{S_0}(\varphi, \omega_0)$  profile at  $\varphi = 90^\circ$  (or  $270^\circ$ ) and  $\varphi = 0^\circ$  (or  $180^\circ$ ) have similar magnitudes, the nature of their appearance is different. The energy barrier at  $\varphi = 0^\circ$  (or  $180^\circ$ ) (planar conformation of ThT) results due to steric interactions of the methyl group of the benzothiazole ring with the hydrogen atoms of the benzene fragment, whereas the barrier at  $\varphi = 90^\circ$  (or  $270^\circ$ ) (twisted conformation of ThT) is caused by the weakening of interactions between  $\pi$  systems of fragment I and fragments II and III. It is noteworthy that positive charge is localized mainly on the benzothiazole ring (fragment I), in particular, for a twisted conformation with  $\varphi = 90^\circ$  (or  $270^\circ$ ). As follows from ab initio RHF/3-21G calculations (Figure 3D), twisting of ThT along the C6–C12 bond results in the growth of total charge of the benzothiazole from  $+0.6e$  ( $\varphi = 0^\circ$ ) to  $+0.7e$  ( $\varphi = 37^\circ$ ) and  $+0.8e$  ( $\varphi = 90^\circ$ ).

Taking into account a rather low contribution of the dimethylamino group in the frontier molecular orbitals of ThT (Figure 4), we further considered only the effect of the torsion

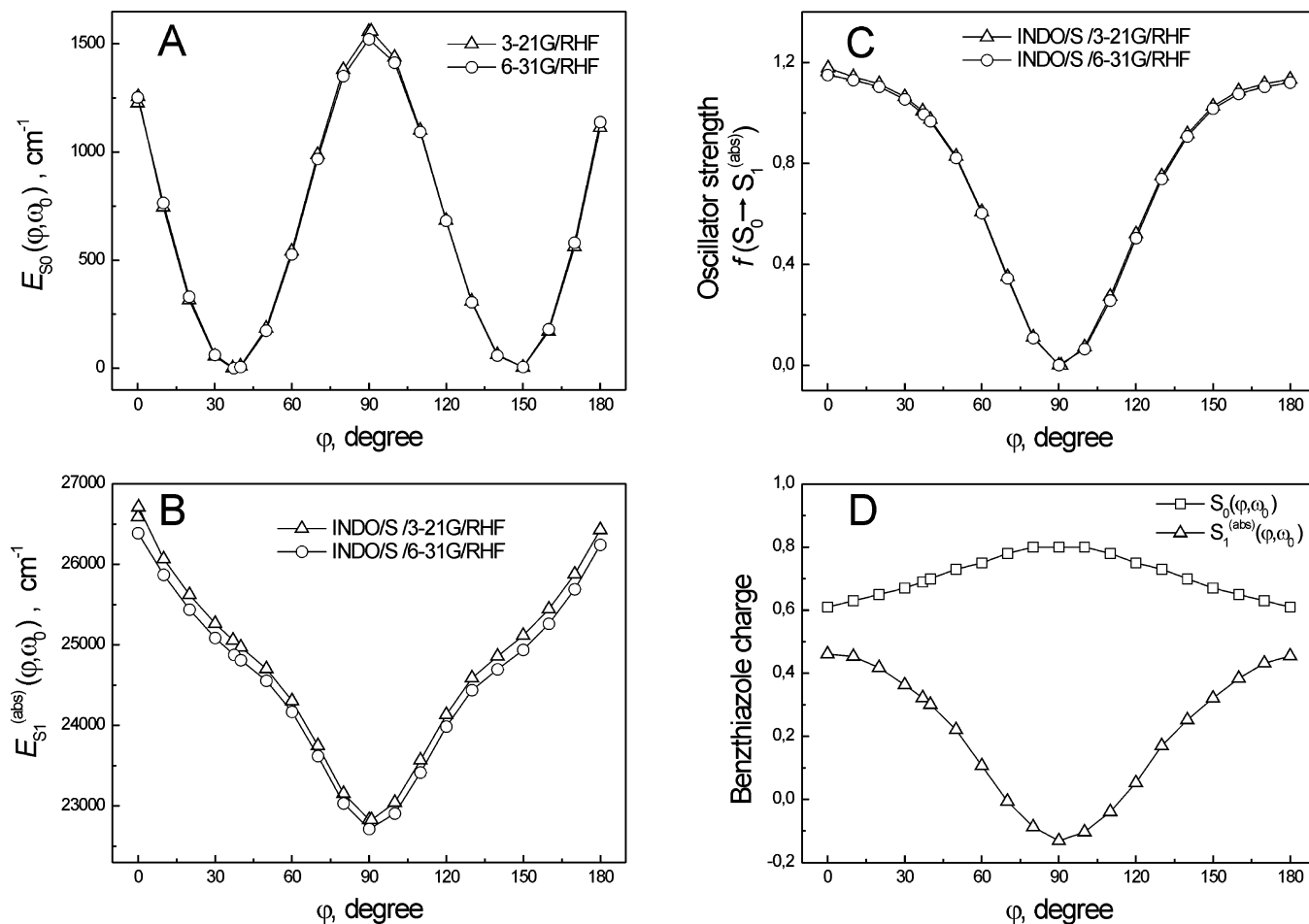


**Figure 3.** Properties of the ground  $S_0$  and first excited state  $S_1^{(abs)}$  for conformers with different  $\varphi$  angles. Conformer geometries and other ground state properties were calculated by ab initio methods using basis sets 3-21G and 6-31G. Properties of the first excited state were obtained using INDO/S method. (A) Energy of the ground  $S_0$  state. (B) Energy of the first excited state  $S_1^{(abs)}$ . (C) Oscillator strength for the first electronic transition  $S_0 \rightarrow S_1^{(abs)}$  calculated with INDO/S method. (D) Total charge of benzthiazole fragment in the ground  $S_0$  and first excited  $S_1^{(abs)}$  states. Conformer geometries were optimized using 3-21G basis set. Charge-transfer  $\Delta Z_{\text{INDO}}$  between fragments upon transition to the excited state was calculated using INDO/S, and the benzthiazole charge in  $S_1^{(abs)}$  state was computed as  $Z(S_1^{(abs)}) = Z(S_0) + \Delta Z_{\text{INDO}}$ .

angle  $\varphi$  (i.e., effect of fragment I and fragment II mutual rotation) on the position of energy levels and other properties of the molecule. Therefore, it is reasonable to include the variable torsion angle  $\psi$  into the set of parameters  $\omega$ .

The INDO/S method was used to determine the energy of electron transition to the Franck–Condon  $S_1^{(abs)}$  state, the first excited singlet state, which resulted immediately after photon absorption. In these calculations, geometries of the conformers in the ground state  $S_0$  obtained by ab initio methods with basis sets 3-21G and 6-31G were used. The energy of the Franck–Condon state  $E_{S_1^{(abs)}}(\varphi, \omega_0)$  of ThT was determined as a sum of the energy in the ground state,  $E_{S_0}(\varphi, \omega_0)$ , obtained by ab initio methods, and the energy difference between  $S_0$  and  $S_1^{(abs)}$  levels,  $\Delta E_{\text{INDO}}(\varphi, \omega_0)$ , calculated by the INDO/S method. Figure 3B represents the dependence of the  $E_{S_1^{(abs)}}(\varphi, \omega_0)$  level position on the torsion angle  $\varphi$ . One can see that the energy of the Franck–Condon state has a minimal value for the twisted conformation of ThT with  $\varphi = 90^\circ$ . Application of wider basis set (6-31G) resulted in only a slight shift in energy of the  $S_1^{(abs)}$  level, and qualitative characteristics of the curve remained invariable. The data obtained allow us to suggest that after transition of ThT to the excited  $S_1^{(abs)}$  state, the torsion angle  $\varphi$  will rise from 37 to  $90^\circ$ , and the molecule will tend to adopt a new conformation with twisted benzthiazole and benzene rings. However, it should be mentioned that the dependence of the  $S_1$  state energy (but not of the  $S_1^{(abs)}$  state) on nuclear coordinates

(more precisely on  $\varphi$  and  $\omega_1$ ) is needed to predict real conformational changes in the excited state. It is reasonable that this dependence may be determined as  $E_{S_1} = E_{S_1}(\varphi, \omega_1)$ , where  $E_{S_1}(\varphi, \omega_1)$  has to be obtained according to the previously mentioned procedure utilized to calculate the  $S_0$  state properties.

However, even now, one can note that the character of the excited  $S_1$  state properties' dependence on angle  $\varphi$  will be significantly different from the character correspondent to the ground  $S_0$  state. Indeed, shapes of the highest occupied molecular orbital (HOMO) and the lowest unoccupied molecular orbital (LUMO) for the ThT conformers depend significantly on the angle  $\varphi$ , and their localization on fragments I–III is changed greatly (Figure 4). One can expect this result since conjugation between the  $\pi$  electronic systems of the fragments I and II at  $\varphi = 0^\circ$  (saddle point) or nearly  $\varphi = \sim 37^\circ$  (potential energy minimum) completely disappears when  $\varphi$  is equal to  $90^\circ$ . This indicates that energy surfaces of the  $S_0(\varphi, \omega_0)$  and  $S_1(\varphi, \omega_1)$  states must have essentially different features and that electronic transitions to the excited state will be accompanied by significant charge transfer among ThT fragments (Figure 3D).

As it was mentioned earlier, for the molecule in the ground  $S_0$  state, a positive charge is localized mainly on the benzthiazole cycle (fragment I), and its value increases from  $Z = +0.6e$  to  $+0.8e$  upon angle  $\varphi$  growth from 0 to  $90^\circ$  (i.e., upon the ThT rings twisting). Transition to the excited  $S_1^{(abs)}$  state results in redistribution of electron density and the transfer of negative

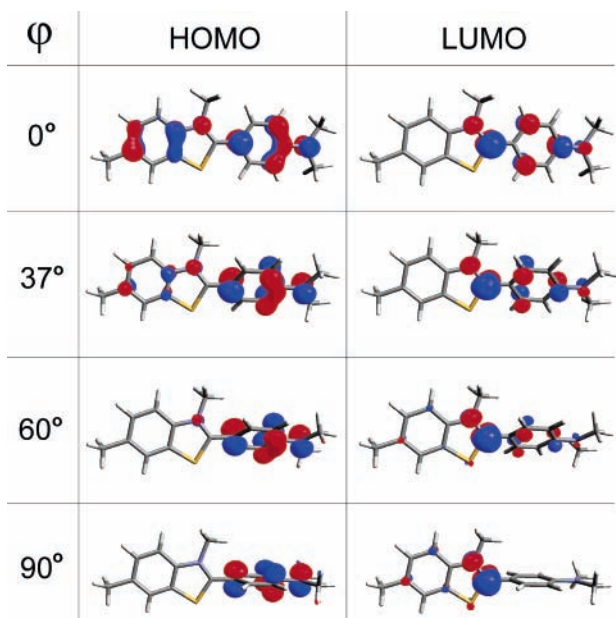


**Figure 4.** HOMO and LUMO of ThT conformers with different angles  $\varphi$  between rings. Orbital shapes were calculated using INDO/S method for conformers with geometries optimized by RHF/3-21G. Negative and positive values of wavefunctions are depicted in red and blue.

charge to fragment I (Figure 3D). It is noteworthy that the magnitude of the transferred charge increases with angle  $\varphi$  growth from 0 to 90° and that the overall benzthiazole (fragment I) charge in the Franck–Condon  $S_1^{(\text{abs})}$  state decreases from  $Z = +0.45e$  (planar conformation) to  $-0.1e$  (twisted conformation). This indicates that intramolecular charge transfer occurs in the excited singlet state  $S_1^{(\text{abs})}$  of ThT upon rotation of the torsion angle  $\varphi$  from 37 to 90° and that this process is favorable in energy (Figure 3B,D).

Importantly, the common domain of localization of the HOMO and LUMO is negligible for the twisted conformation of ThT with torsion angle  $\varphi = 90$  or  $270^\circ$  (Figure 4 and Table 2). As a result, the oscillator strength for an electronic transition between the  $S_0$  and the  $S_1^{(\text{abs})}$  states (Figure 3C) is close to zero for the twisted conformation (i.e., this state is nonfluorescent since optical transition is forbidden).

To obtain the energy surface  $E_{S_1}(\varphi, \omega_1)$ , geometries of the ThT conformers with fixed  $\varphi$  values in the first excited-state were optimized using the CIS/RHF/3-21G method (Supporting Information). As it was already mentioned, the CIS method significantly overestimates the energies of the excited states; however, predicted geometries are quite reasonable. In the case of ThT, the calculated energies of the  $S_1(\varphi, \omega_1)$  state were also considerably higher than expected. The minimum on the potential energy  $E_{S_1}(\varphi, \omega_1)$  profile was observed at  $\varphi \sim 21^\circ$

in contrast to results for the non-relaxed state  $S_1^{(\text{abs})}(\varphi, \omega_0)$ , where energy was minimal at 90°. However, it must be noted that the error of energy overestimation by the CIS method was higher than the variation of  $E_{S_1}(\varphi, \omega_1)$  values on the  $\varphi$  angle (Table 2).

Therefore, the INDO/S method was used again to determine energies of conformers with geometries optimized in the excited state. Initially, the ab initio method was utilized to obtain the energy  $E_{S_0}(\varphi, \omega_1)$  of the ground state. Then, for a given geometry, the energy difference  $\Delta E_{\text{INDO}}(\varphi, \omega_1)$  between  $S_0$  and  $S_1$  levels was calculated by the INDO/S method. Obtained dependence  $E_{S_1^{(\text{fluor})}}(\varphi, \omega_1) = E_{S_0}(\varphi, \omega_1) + \Delta E_{\text{INDO}}(\varphi, \omega_1)$  (Figure 5) has a minimum at  $\varphi = \sim 80\text{--}100^\circ$  in accordance with the energy of the  $S_1^{(\text{abs})}(\varphi, \omega_0)$  level but not at  $\varphi \sim 21^\circ$  as predicted by the CIS method. At the same time, the  $E_{S_1^{(\text{fluor})}}(\varphi, \omega_1)$  curve has a plateau for angle  $\varphi$  values ranging from 20 to 50° (Figure 5), and taking into account the data of ab initio CIS calculations, we cannot exclude the possibility of a shallow minimum existence in this region.

Obtained dependences of oscillator strength for the electronic transition  $S_1^{(\text{fluor})}(\varphi, \omega_1) \rightarrow S_0(\varphi, \omega_1)$  and of the benzthiazole charge on the torsion angle  $\varphi$  (Figure 6) are similar to those for the Franck–Condon  $S_1^{(\text{abs})}(\varphi, \omega_0)$  state (Figure 3). One can see that a significant change of molecular properties occurs upon ThT fragments twisting with a deflection point of  $\varphi = \sim 60^\circ$ . It is noteworthy that the oscillator strength of the electron transition changes its magnitude from  $f = \sim 0.8\text{--}1.0$  ( $\varphi$  ranges from 0 to 50°) to  $f = \sim 0$  ( $\varphi$  ranges from 70 to 90°). Thus, twisting of the molecule leads to alteration of the lowest excited state nature, and two different types of electronic states can be distinguished. Taking into account charge redistribution character between ThT fragments, which takes place in the excited state (Figures 3D and 6B) as compared to the ground state, it is suitable to denote these states as the LE state ( $\varphi = \sim 0\text{--}50^\circ$  and  $f = \sim 0.8\text{--}1.0$ ) and the TICT state ( $\varphi = \sim 70\text{--}90^\circ$  and  $f = \sim 0$ ).

Thus, taking into account the features of  $E_{S_0}(\varphi, \omega_0)$ ,  $E_{S_1^{(\text{abs})}}(\varphi, \omega_0)$ , and  $E_{S_1^{(\text{fluor})}}(\varphi, \omega_1)$  dependences, the following model of photophysical processes in the ThT molecule may be suggested (Figure 5). A rather low ( $\sim 700\text{--}1500\text{ cm}^{-1}$  depending on the calculation method) barrier of fragments I and II mutual rotation separates several nonplanar conformers of similar energy with torsion angles  $\varphi = \sim 37, 145, 217, \text{ or } 325^\circ$ . These conformers can be effectively excited to the  $S_1^{(\text{abs})}$  level by a photon, and the oscillator strength for the corresponding  $S_0 \rightarrow S_1^{(\text{abs})}$  transition is high (Figure 3C). Further relaxation of the Franck–Condon state  $S_1^{(\text{abs})}$  results in geometry alteration of the molecule in the excited state (i.e., changes of torsion angle  $\varphi$  and the set of geometrical parameters  $\omega$ ).

Consider photoexcitation of the conformer with  $\varphi = \sim 37^\circ$ . One can distinguish two relaxational processes in the excited

**TABLE 2: Molecular Properties for Selected ThT Conformers in Ground and Excited Singlet States**

	method	$\varphi = 0^\circ$	$\varphi = 37^\circ$	$\varphi = 90^\circ$
$E_{S_0}(\varphi, \omega_0) - E_{S_0}(\varphi = 37^\circ, \omega_0)$ ( $\text{cm}^{-1}$ )	RHF/3-21G	1250	0	1560
$\mu(S_0(\varphi, \omega_0))$ (D)	RHF/3-21G	3.8	3.1	3.1
$E_{S_1}(\varphi, \omega_0) - E_{S_0}(\varphi, \omega_0)$ ( $\text{cm}^{-1}$ )	CIS/RHF/3-21G	35120	36140	38940
$E_{S_1^{(\text{abs})}}(\varphi, \omega_0) - E_{S_0}(\varphi, \omega_0)$ ( $\text{cm}^{-1}$ )	INDO/S	25360	25060	21270
$\mu(S_1(\varphi, \omega_0))$ (D)	CIS/RHF/3-21G	5.4	7.0	14.4
oscillator strength $f(S_0(\varphi, \omega_0) \rightarrow S_1^{(\text{abs})}(\varphi, \omega_0))$	INDO/S	1.16	1.01	0.00
$E_{S_1}(\varphi, \omega_1) - E_{S_0}(\varphi, \omega_1)$ ( $\text{cm}^{-1}$ )	CIS/RHF/3-21G	30790	32710	27910
$E_{S_1^{(\text{fluor})}}(\varphi, \omega_1) - E_{S_0}(\varphi, \omega_1)$ ( $\text{cm}^{-1}$ )	INDO/S	21670	23010	13210
$\mu(S_1(\varphi, \omega_1))$ (D)	CIS/RHF/3-21G	4.4	5.9	13.7
$E_{S_0}(\varphi, \omega_1) - E_{S_0}(\varphi = 37^\circ, \omega_0)$ ( $\text{cm}^{-1}$ )	RHF/3-21G	3800	1730	7620
oscillator strength $f(S_0(\varphi, \omega_1) \rightarrow S_1^{(\text{fluor})}(\varphi, \omega_1))$	INDO/S	0.88	1.00	0.00 (for $\varphi = 80^\circ$ )
$\mu(S_0(\varphi, \omega_1))$ (D)	RHF/3-21G	4.9	4.0	2.8

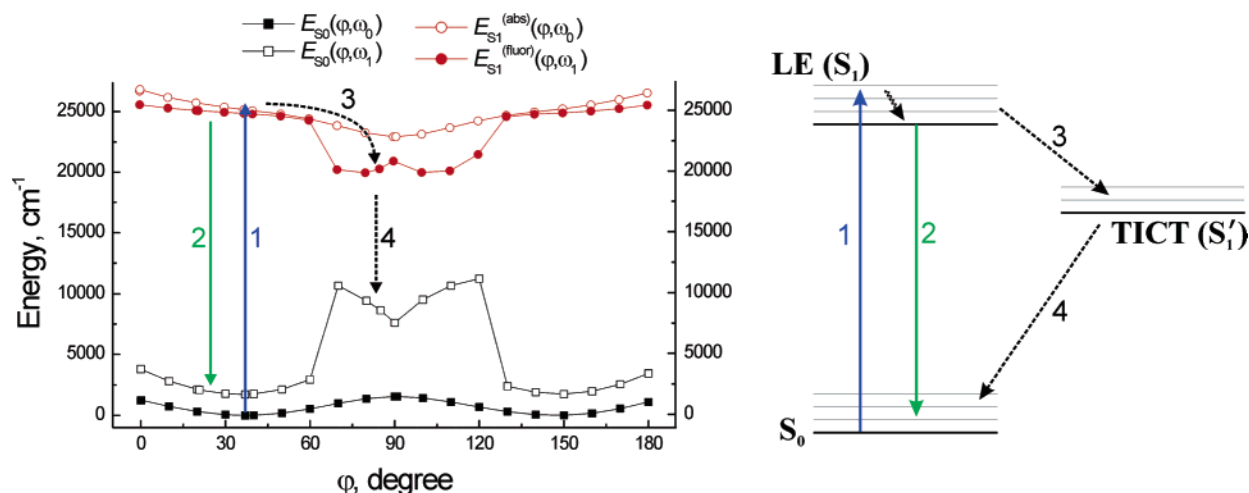


**Figure 5.** (Left) Energy dependence of  $E_{S_0}(\varphi, \omega_0)$ ,  $E_{S_0}(\varphi, \omega_1)$ ,  $E_{S_1}^{(abs)}(\varphi, \omega_0)$ , and  $E_{S_1}^{(fluor)}(\varphi, \omega_1)$  states on torsion angle  $\varphi$ . Geometries of conformers were optimized using 3-21G basis set. Arrows denote absorption (1), fluorescence from LE state (2), torsional relaxation process from LE to TICT state (3), and nonradiative transition from TICT state to the ground state (4). (Right) Scheme of excitation energy deactivation in ThT molecule.

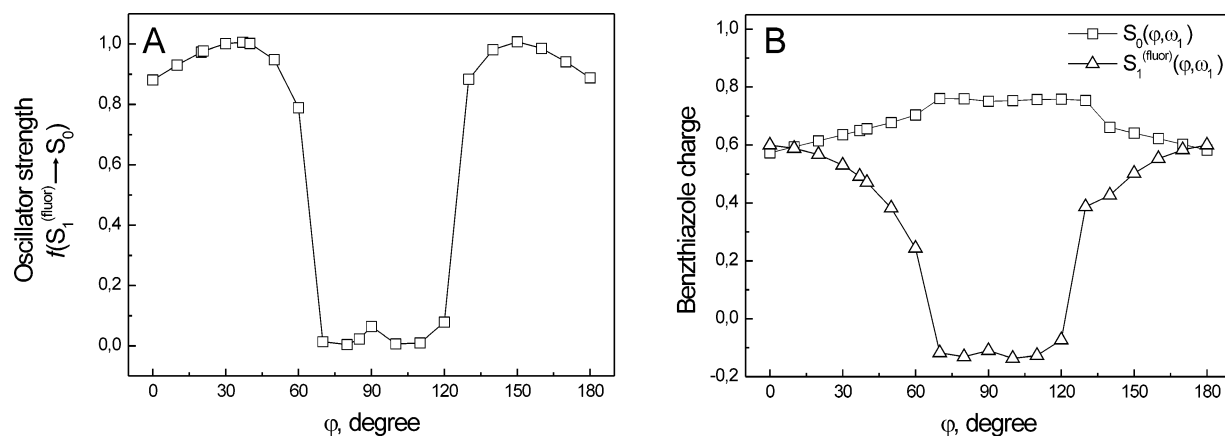


**Figure 6.** (A) Oscillator strength for the first electronic transition  $S_1^{(fluor)} \rightarrow S_0$  calculated with INDO/S method. (B) Total charge of benzthiazole fragment in the excited  $S_1^{(fluor)}(\varphi, \omega_1)$  and ground  $S_0(\varphi, \omega_1)$  states. Conformer geometries in the excited state were optimized using CIS/RHF/3-21G method. Charge-transfer  $\Delta Z_{INDO}$  between fragments upon transition to the excited state was calculated using INDO/S. Benzthiazole charge in  $S_1^{(fluor)}$  state was computed as  $Z(S_1^{(fluor)}) = Z(S_0) + \Delta Z_{INDO}$ .

state. First, a fast transformation corresponding to changes  $\omega_0 \rightarrow \omega_1$  at constant  $\varphi \approx 37^\circ$ . Second, a rather slow transformation of the torsion angle along two routes: (1) change  $\varphi \approx 37^\circ \rightarrow \varphi \approx 21^\circ$  leading to the production of a relaxed LE state and (2) change  $\varphi \approx 37^\circ \rightarrow \varphi \approx 90^\circ$  resulting in TICT state formation (presented values of the angles are approximate). This separation of relaxational processes is reasonable since twisting of the molecule fragments will require much more time than changes of bond lengths or linear angles between atoms.

Let us assume that only a fast relaxational process takes place (i.e., change  $\omega_0 \rightarrow \omega_1$  at constant  $\varphi \approx 37^\circ$ ). Experimentally observed fluorescence from the LE state corresponds to the transition  $S_1^{(fluor)}(\varphi \approx 20-40^\circ, \omega_1) \rightarrow S_0(\varphi \approx 20-40^\circ, \omega_1)$ , and according to the calculations (Figure 5), the Stokes shift will be determined mainly by the difference of the ground state energy levels  $E_{S_0}(\varphi, \omega_1) - E_{S_0}(\varphi, \omega_0)$ . The estimated value of the Stokes shift  $\sim 2000 \text{ cm}^{-1}$  agrees rather well with the experimental one  $\sim 3200-4000 \text{ cm}^{-1}$  (Supporting Information). Better quantitative agreement probably could be achieved if calculations were performed taking into account the solvation effects. The value of the dipole moment change upon photoexcitation  $\Delta\mu = 4.6 \pm 0.7 \text{ D}$  (see Supporting Information) obtained using the Lippert–Mataga equation<sup>50</sup> (radius of Onsager cavity for ThT was assumed to be  $a = 3 \text{ \AA}$ ) agrees well with the calculated  $\mu(S_1(\varphi = 37^\circ, \omega_1)) - \mu(S_0(\varphi = 37^\circ, \omega_0))$

$= 3.8 \text{ D}$ . This mechanism of photophysical transformations will be typical for ThT in viscous solvents where twisting of the molecular fragments is hindered.

For the case of non-viscous solvents, a transition from the initial ( $\varphi \approx 37^\circ$ ) to the twisted conformation ( $\varphi \approx 90^\circ$ ) will take place in the excited state, resulting in a practically nonfluorescent TICT state with oscillator strength  $f(S_1 \rightarrow S_0) \approx 0$ . This process effectively competes with radiative transition from the LE state and is responsible for significant quenching of ThT fluorescence in low-viscosity solvents.

When the ThT molecule is located in a rather rigid microenvironment, for example, when it is bound to amyloid fibrils, twisting of the dye is blocked due to steric hindrance, which results in elimination of the quenching process and a rise of fluorescence intensity. Therefore, only dyes incorporated into amyloid fibrils possess a significant QY of emission, and fluorescence of nonbound ThT is negligible.

The absence of additional experimental information does not permit us to make any reliable conclusions about further nonradiative deactivation of the TICT state. Nevertheless, it can be noted that the energy difference  $E_{S_1^{(fluor)}}(\varphi = 90^\circ, \omega_1) - E_{S_0}(\varphi = 90^\circ, \omega_1)$  is rather small ( $\sim 10\,000 \text{ cm}^{-1}$ ) and possibly even lower if the influence of polar solvents will be taken into consideration. Significant dipole moment of the  $S_1^{(fluor)}(\varphi = 90^\circ, \omega_1)$  state (Table 2) may result in additional stabilization of

the energy level in polar solvents giving the situation when the conical intersection of  $S_1(\text{fluor})(\varphi = 90^\circ, \omega_1)$  and  $S_0(\varphi = 90^\circ, \omega_1)$  levels occurs. The latter may promote quite rapid nonradiative deactivation of the excited TICT state. This indicates that further quantum-chemical calculations that take into account the influence of the polar environment on the ThT properties are of great interest.

## Conclusion

On the basis of the quantum-chemical calculation results, the scheme of the photophysical processes in the excited  $S_1$  state of the ThT molecule is suggested. The data obtained confirm that ThT behaves as a molecular rotor and that fluorescent properties of the dye molecule can be successfully explained in the framework of the following model. According to it, the TICT process takes place for the ThT molecule in the excited singlet state, and the angle between benzothiazole and benzene rings changes from 37 to  $90^\circ$ , resulting in a transition from fluorescent LE state to nonfluorescent TICT state. This process effectively competes with the radiative transition from the LE state and is responsible for significant quenching of ThT fluorescence in low-viscosity solvents. On the contrary, for viscous solvents or when ThT is located in a rather rigid microenvironment, for example, when it is bound to amyloid fibrils, internal rotation in the dye molecule is blocked due to steric hindrance, which results in a high QY of fluorescence due to the suppression of the LE  $\rightarrow$  TICT quenching process.

**Acknowledgment.** This work was supported by the Belarusian Republican Foundation for Fundamental Research (Grants F06-351 and XO6P-115), the Russian Foundation of Basic Research (06-04-81033 and 07-04-01454), the Program "Molecular and Cell Biology" RAS, and the Program "Leading Scientific Schools of Russia" (9396.2006.4). The authors are grateful to Prof. K. N. Solov'yov and Dr. V. N. Uversky for valuable discussions.

**Supporting Information Available:** Additional computational details, dipole moments and structures of conformers, graph of dipole moment vs torsion angle and of Stokes shift vs solvent orientational polarizability,  $\Delta f$ , and Cartesian geometries of the structures. This material is available free of charge via the Internet at <http://pubs.acs.org>.

## References and Notes

- Selkoe, D. J. *Nature* **2003**, *426*, 900–904.
- Fink, A. L. *Fold Des.* **1998**, *3*, 9–23.
- Zerovnik, E. *Eur. J. Biochem.* **2002**, *269*, 3362–3371.
- Harper, J. D.; Lieber, C. M.; Lansbury, P. T., Jr. *Chem. Biol.* **1997**, *4*, 951–959.
- Carrell, R. W.; Gooptu, B. *Curr. Opin. Struct. Biol.* **1998**, *8*, 799–809.
- Koo, E. H.; Lansbury, P. T., Jr.; Kelly, J. W. *Proc. Natl. Acad. Sci. U.S.A.* **1999**, *96*, 9989–9990.
- Naiki, H.; Higuchi, K.; Hosokawa, M.; Takeda, T. *Anal. Biochem.* **1989**, *177*, 244–249.
- LeVine, H., III. *Protein Sci.* **1993**, *2*, 404–410.
- LeVine, H., III. *Methods Enzymol.* **1999**, *309*, 274–284.
- Yoshiike, Y.; Chui, D. H.; Akagi, T.; Tanaka, N.; Takashima, A. *J. Biol. Chem.* **2003**, *278*, 23648–23655.
- Ilanchelian, M.; Ramaraj, R. *J. Photochem. Photobiol., A* **2004**, *162*, 129–137.
- Raj, C. R.; Ramaraj, R. *Photochem. Photobiol.* **2001**, *74*, 752–759.
- Khurana, R.; Coleman, C.; Ionescu-Zanetti, C.; Carter, S. A.; Krishna, V.; Grover, R. K.; Roy, R.; Singh, S. *J. Struct. Biol.* **2005**, *151*, 229–238.
- Voropay, E. S.; Samtsov, M. P.; Kaplevsky, K. N.; Maskevich, A. A.; Stepuro, V. I.; Povarova, O. I.; Kuznetsova, I. M.; Tutoverov, K. K.; Fink, A. L.; Uversky, V. N. *J. Appl. Spectrosc.* **2003**, *70*, 868–874.
- Friedhoff, P.; Schneider, A.; Mandelkow, E. M.; Mandelkow, E. *Biochemistry* **1998**, *37*, 10223–10230.
- Maskevich, A. A.; Stsiapura, V. I.; Kuzmitsky, V. A.; Kuznetsova, I. M.; Povarova, O. I.; Uversky, V. N.; Turoverov, K. K. *J. Proteome Res.* **2007**, *6*, 1392–1401.
- Lindgren, M.; Sorgjerd, K.; Hammarstrom, P. *Biophys. J.* **2005**, *88*, 4200–4212.
- Loutfy, R. O.; Arnold, B. A. *J. Phys. Chem.* **1982**, *86*, 4205–4211.
- Loutfy, R. O. *Pure Appl. Chem.* **1986**, *58*, 1239–1248.
- Valeur, B. *Molecular Fluorescence: Principles and Applications*; Wiley-VCH Verlag GmbH: New York, 2001.
- Allen, B. D.; Benniston, A. C.; Harriman, A.; Rostron, S. A.; Yu, C. *Phys. Chem. Chem. Phys.* **2005**, *7*, 3035–3040.
- Haidekker, M. A.; Brady, T. P.; Lichlyter, D.; Theodorakis, E. A. *Bioorg. Chem.* **2005**, *33*, 415–425.
- Dewar, M. J. S.; Zebisch, E. G.; Healy, E. F.; Stewart, J. J. P. *J. Am. Chem. Soc.* **1985**, *107*, 3902–3909.
- Stewart, J. J. P. *J. Comput. Chem.* **1989**, *10*, 221–264.
- Binkley, J. S.; Pople, J. A.; Hehre, W. J. *J. Am. Chem. Soc.* **1980**, *102*, 939–947.
- Hehre, W. J.; Ditchfield, R.; Pople, J. A. *J. Chem. Phys.* **1972**, *56*, 2257–2261.
- Hariharan, P. C.; Pople, J. A. *Theor. Chim. Acta* **1973**, *28*, 213–222.
- Frisch, M. J.; Head-Gordon, M.; Pople, J. A. *Chem. Phys. Lett.* **1990**, *166*, 275–280.
- Foresman, J. B.; Head-Gordon, M.; Pople, J. A.; Frisch, M. J. *J. Phys. Chem.* **1992**, *96*, 135–149.
- Schmidt, M. W.; Gordon, M. S. *Ann. Rev. Phys. Chem.* **1998**, *49*, 233–266.
- Kowalski, K.; Piecuch, P. *J. Chem. Phys.* **2004**, *120*, 1715–1738.
- Stanton, J. F.; Gauss, J.; Ishikawa, N.; Head-Gordon, M. *J. Chem. Phys.* **1995**, *103*, 4160–4174.
- Shukla, M. K.; Leynski, J. *J. Phys. Chem. A* **2002**, *106*, 1011–1018.
- Sobolewski, A. L.; Domcke, W. *Phys. Chem. Chem. Phys.* **1999**, *1*, 3065–3072.
- Scheiner, S. *J. Phys. Chem. A* **2000**, *104*, 5898–5909.
- Mishra, S. K.; Mishra, P. C. *Spectrochim. Acta, Part A* **2001**, *57*, 2433–2450.
- Gittins, C. M.; Rohlfling, E. A.; Rohlfling, C. M. *J. Chem. Phys.* **1996**, *105*, 7323–7335.
- Luth, K.; Scheiner, S. *J. Phys. Chem.* **1994**, *98*, 3582–3587.
- Wiberg, K. B.; Wang, Y. *J. Phys. Chem. A* **2004**, *108*, 9417–9422.
- Wiberg, K. B. et al. *J. Phys. Chem. A* **2005**, *109*, 466–477.
- Parusel, A. B. J.; Rettig, W.; Sudholt, W. *J. Phys. Chem. A* **2002**, *106*, 804–815.
- Grabowski, Z. R.; Rotkiewicz, K.; Rettig, W. *Chem. Rev.* **2003**, *103*, 3899–4031.
- Zerner, M. C.; Loew, G. H.; Kirchner, R. F.; Mueller-Westerhoff, U. T. *J. Am. Chem. Soc.* **1980**, *102*, 589–599.
- Kuzmitsky, V. A. *Preprint of the Institute of Physics BSSR Acad. Sci.* **1979**, *188*, 1–49 (in Russian).
- Luzanov, A. V. *Usp. Khim.* **1980**, *49*, 2086–2117 (in Russian).
- Nemukhin, A. V.; Grigorenko, B. L.; Granovsky, A. A. *Moscow Univ. Chem. Bull.* **2004**, *45*, 75–102.
- Schmidt, M. W.; Baldrige, K. K.; Boatz, J. A.; Elbert, S. T.; Gordon, M. S.; Jensen, J. J.; Koseki, S.; Matsunaga, N.; Nguyen, K. A.; Su, S.; Windus, T. L.; Dupuis, M.; Montgomery, J. A. *J. Comput. Chem.* **1993**, *14*, 1347–1363.
- Portmann, S.; Luthi, H. P. *Chimia* **2000**, *54*, 766–770.
- ArgusLab 4.0.1*; Mark A. Thompson Planaria Software LLC: Seattle, WA; <http://www.arguslab.com>.
- Lakowicz, J. R. *Principles of Fluorescence Spectroscopy*, 2nd ed.; Kluwer Academic/Plenum Publishers: New York, 1999.